J. Fluid Mech. (1981), *vol.* 108, *pp.* 227–240
Printed in Great Britain

Computation of the flow between two rotating coaxial disks: multiplicity of steady-state solutions

By M. HOLODNIOK,† M. KUBÍČEK and V. HLAVÁČEK

Department of Chemical Engineering, Prague Institute of Chemical Technology, 16628 Praha 6, Czechoslovakia

(Received 12 February 1980 and in revised form 14 October 1980)

A numerical investigation of the problem of rotating disks is made using the Newton–Raphson and continuation methods. The numerical analysis of the problem was performed for a sequence of values of the Reynolds number R and the ratio of angular velocities of both disks s. It was shown that for higher values of the Reynolds number it is necessary to use a large number of grid points. Continuation of the solution with respect to the parameter s indicated that a number of branches may exist. A detailed discussion for three selected values of s ($s = -1$, $s = 0$, $s = 1$) is presented together with a detailed comparison of our calculations with results already published in the literature.

1. Introduction

The paper is a continuation of our previous work (Holodniok, Kubíček & Hlaváček 1977). We shall consider only the steady-state description of the physical situation, the transient behaviour will be a subject of our next paper.

The purposes of this paper are (i) to perform numerical calculation for higher values of the Reynolds number and to test the capability of the finite-difference approach; (ii) for a given value of the Reynolds number to calculate the dependence of the solution on the value of the parameter s; and (iii) to compare our calculations with the results published in the literature.

The steady-state formulation of the problem is ($' = d/d\xi$)

$$\left.\begin{aligned} F'' &= R^{\frac{1}{2}}HF' + R(F^2 - G^2 + k), \\ G'' &= 2RFG + R^{\frac{1}{2}}G'H, \\ H' &= -2R^{\frac{1}{2}}F. \end{aligned}\right\} \tag{1}$$

The boundary conditions are

$$\left.\begin{aligned} F(0) = H(0) = 0, \quad G(0) = 1, \\ F(1) = H(1) = 0, \quad G(1) = s. \end{aligned}\right\} \tag{2}$$

Here s is a parameter which represents the ratio of velocities of both disks, $-1 \leqslant s \leqslant 1$, and R is the Reynolds number. We have to calculate the profiles $F(\xi)$, $G(\xi)$, $H(\xi)$ for $\xi \in [0, 1]$ and the nonlinear eigenvalue k, which fulfil equations (1) and (2).

The problem of the flow of a viscous fluid between two rotating disks has been a

† Computer Centre, Prague Institute of Chemical Technology.

subject of many papers. Unfortunately the governing equations have been written in different variables. Table 1 is presented in order to make it possible to transform the results between different formulations.

We shall show that for higher values of the parameter R a large number of solutions can be found. The dependence on the parameter s is presented for one selected value of the Reynolds number. The results obtained will be discussed in connection with the calculations published in the literature.

2. Computational method

A number of different numerical methods have been adapted to solve the problem of two infinite rotating disks. A discussion of these techniques has been published recently (Holodniok *et al.* 1977). From this discussion it may be inferred that for higher values of R the most powerful approach is the finite-difference method. The simple-shooting method fails; however, the multiple-shooting algorithm has been successfully used by Pesch & Rentrop (1978) for values ranging up to $R = 20000$.

The finite-difference approximation of equations (1) and (2), used in this study, has been described in our previous paper (Holodniok *et al.* 1977). The derivatives are replaced by three-point difference formulae; the error of approximation is $O(h^2)$, where $h = 1/n$ is the step used for finite-difference formulae. The finite-difference approximation is represented by a system of $3(n-1)+1$ nonlinear algebraic equations with almost seven-diagonal structural matrix. The Newton–Raphson method has been used to solve this system for particular values of the parameters R and s. By using the Newton–Raphson method sequentially we can obtain a dependence of the solution on R. Let us discuss an appropriate number of the grid points for different values of R. For higher values of R it is necessary to consider the results with some care. Such a situation is depicted in figure 1, where the dependence of k on R for different n is presented. This figure reveals that for $R > 1000$ the results obtained for $n = 100$ and $n = 200$ are different. For $R > 4000$ it is desirable to use $n = 400$ for certain branches. The detailed situation is demonstrated on figure 2, where two further branches, 7 and 9, of the solution are presented. We can expect that for $R > 1000$ a grid having $n = 800$ is not sufficient. We can, however, obtain a parasitic solution for higher R and low n (cf. branch 7, $n = 100$, $R \sim 5000$), which for higher n disappears. It is our opinion that for higher values of R the multiple-shooting technique is the best method (cf. Schlehöferová, Holodniok & Kubíček 1981). We shall perform a systematic analysis of a dependence of the solution on the parameter s. The value of R was fixed at $R = 625$, because for low values of R it is not necessary to use a very dense grid and $n = 200$ is sufficient. Moreover, with increasing R the number of solutions increases and the overall picture can be very complex. Let us note that the seven branches drawn in figures 1 and 2 do not represent all solutions of the problem for $R = 625$; a more complete pattern of all branches calculated can be found for $s = 0{\cdot}8$ (see figure 3).

3. Multiplicity and characteristic features of the solution in dependence on s

The dependence of k on s for $R = 625$ is presented in figure 3. Individual branches are numbered according to the order in which they have been obtained. The numbers of the first seven branches coincide with the numbering in figures 1 and 2.

Lance & Rogers (1962)	$F(\xi)$	$G(\xi)$	$H(\xi)$	k	—
Batchelor (1951)	$-\frac{1}{2}h'(\bar{\xi})$	$g(\bar{\xi})$	$h(\bar{\xi})$	$\frac{\Omega^2+c}{\Omega^2}$	$\bar{\xi} = R^{\frac{1}{2}}\xi$
Stewartson (1953)	$\frac{1}{\Omega}H'(\bar{\xi})$	$\frac{1}{\Omega}G(\bar{\xi})$	$\frac{2}{(\nu\Omega)^{\frac{1}{2}}}H(\bar{\xi})$	$\frac{\lambda}{\Omega^2}$	$\bar{\xi} = d(1-\xi)$
Pearson (1965)	$-\frac{1}{2}H'(\xi)$	$G(\xi)$	$R^{\frac{1}{2}}H(\xi)$	—	—
Tam (1969)	$H'(\xi)$	$G(\xi)$	$2R^{\frac{1}{2}}H(\xi)$	—	—
Rasmussen (1971)	$F'(\xi)$	$H(\xi)$	$2R^{\frac{1}{2}}F(\xi)$	—	—
Mellor, Chapple & Stokes† (1968)	$\frac{1}{g(\eta_d)}h'(\eta)$	$\frac{1}{g(\eta_d)}g(\eta)$	$2\frac{1}{[g(\eta_d)]^{\frac{1}{2}}}h(\eta)$	$\frac{\lambda}{[g(\eta_d)]^2}$	$\eta = Re^{\frac{1}{2}}\frac{1}{[g(\eta_d)]^{\frac{1}{2}}}(1-\xi)$
Roberts & Shipman (1976)	$\frac{1}{g(\eta_d)}h'(\eta)$	$\frac{1}{g(\eta_d)}g(\eta)$	$2\frac{1}{[g(\eta_d)]^{\frac{1}{2}}}h(\eta)$	$\frac{\lambda}{[g(\eta_d)]^2}$	$\eta = Re^{\frac{1}{2}}\frac{1}{[g(\eta_d)]^{\frac{1}{2}}}(1-\xi)$
Greenspan (1971)	$-\frac{1}{2}H'(\xi)$	$G(\xi)$	$R^{\frac{1}{2}}H(\xi)$	—	for $\Omega = 1$ and $d = 1$
Schultz & Greenspan (1974)	$-\frac{1}{2}H'(\xi)$	$G(\xi)$	$R^{\frac{1}{2}}H(\xi)$	—	,,
Barrett (1975)	$-\frac{1}{2}H'(\xi)$	$G(\xi)$	$R^{\frac{1}{2}}H(\xi)$	—	,,
McLeod & Parter (1974)	$H'(\bar{\xi})$	$-G(\bar{\xi})$	$-R^{\frac{1}{2}}H(\bar{\xi})$	—	$\bar{\xi} = 2.\xi - 1$
Pesch & Rentrop (1978)	$\frac{2}{R}f'(\bar{\xi})$	$-\frac{2}{R}g(\bar{\xi})$	$-\frac{2}{R^{\frac{1}{2}}}f(\bar{\xi})$	—	$\bar{\xi} = 2.\xi - 1$
Nguyen, Ribault & Florent (1975)	$-\frac{1}{2R}f'(\bar{\xi})$	$\frac{1}{R}g(\bar{\xi})$	$-\frac{1}{R^{\frac{1}{2}}}f(\bar{\xi})$	—	$\bar{\xi} = 1-\xi$

† For computation.

TABLE 1. Transformations between Lance & Rogers' formulation of the problem (used here) and formulations of other authors. (A prime denotes differentiation.)

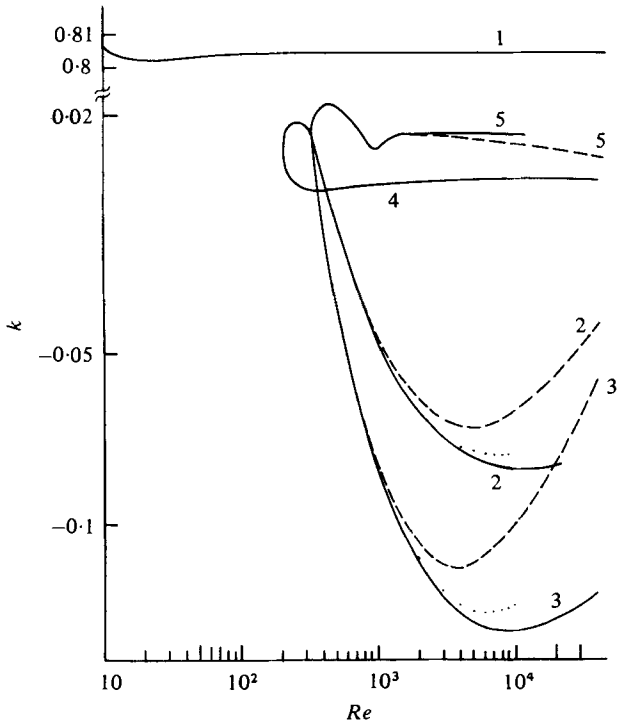

FIGURE 1. Dependence of k on the Reynolds number, $s = 0{\cdot}8$. The effect of n (step size used for finite-difference approximation). – – –, $n = 100$; . . . , $n = 200$; ——, $n = 400$.

Let us study some features of the solution for $s = 1$ and $s = -1$. For $s = 1$ we have the trivial solution of the problem

$$H(\xi) = 0, \quad F(\xi) = 0, \quad G(\xi) = 1, \quad k = 1 \tag{3}$$

(see branch number 1 in figure 3). Suppose that there exists a non-trivial solution $H(\xi)$, $F(\xi)$, $G(\xi)$, k for $s = 1$. Then the functions

$$\tilde{F}(\xi) = F(1-\xi), \quad \tilde{G}(\xi) = G(1-\xi), \quad \tilde{H}(\xi) = H(1-\xi), \quad \tilde{k} = k \tag{4}$$

are also a solution of the problem for $s = 1$. Similarly, suppose that there is a solution $H(\xi)$, $F(\xi)$, $G(\xi)$, k for $s = -1$. Then the functions

$$\tilde{F}(\xi) = F(1-\xi), \quad \tilde{G}(\xi) = -G(1-\xi), \quad \tilde{H}(\xi) = -H(1-\xi), \quad \tilde{k} = k \tag{5}$$

satisfy equations (1) and (2) for $s = -1$, too.

We can take advantage of equations (4) or (5) towards a construction of a new solution for $s = 1$ or $s = -1$, if the new solution is different from the original one. If $\tilde{H} = H, \tilde{F} = F, \tilde{G} = G$, then the solutions will be referred to as the symmetrical profile. Let us note that by using relations (4) branches 10, 14, 3 and 11 arise from branches 7, 9, 2 and 5 for $s = 1$, respectively. Analogously, by using relations (5) we have obtained branches 14, 6, 12, 13, 17 and 19 from branches 9, 3, 1, 10, 15 and 18 for $s = -1$, respectively (cf. figure 3). We incur computational problems in trying to calculate branches 13 and 11 (branch 11 is very close to branch 5 in figure 3 for $s \in [0{\cdot}9, 1]$). We were not able to cross the limit points on these branches by using successive

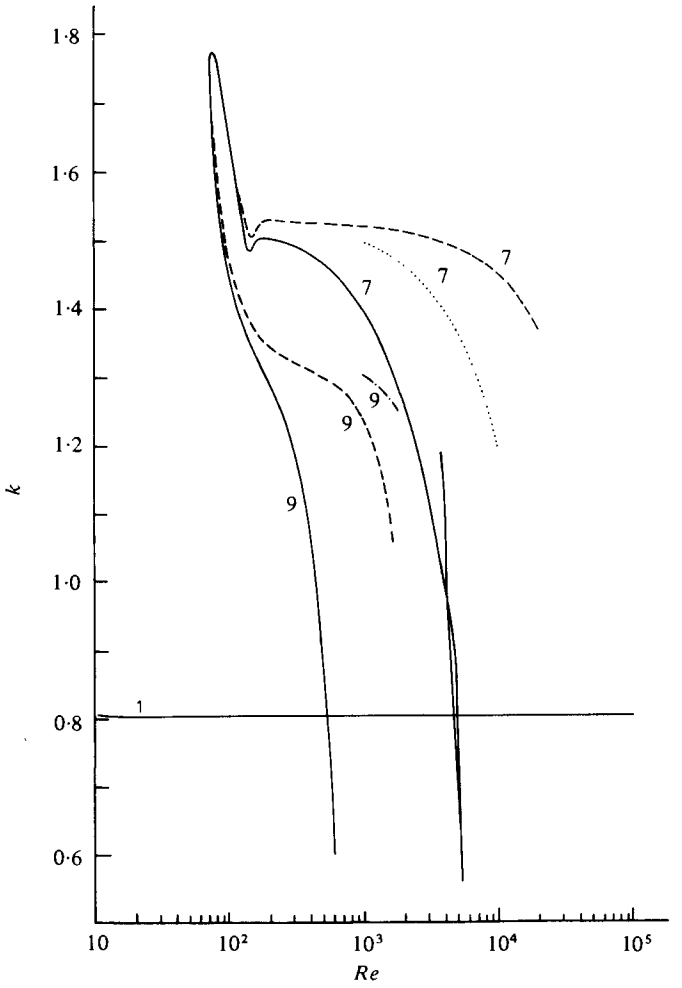

FIGURE 2. Dependence of k on the Reynolds number, $s = 0{\cdot}8$. The effect of n. ——, $n = 100$; . . ., $n = 200$; – – –, $n = 400$; – · – · –, $n = 800$.

changing of s and the finite-difference approach for fixed value of s. However, another procedure allowed us to compute branches 16, 15, 18 and 20 after calculating branches 11, 13, 17 and 19, respectively. This procedure consisted in using the finite-difference approach for a fixed value of k and evaluating the dependence $s = s(k)$.

For $s = 0{\cdot}8$ we calculated ten solutions; the branches 1–5 are continued in R in figure 1 only.

Mellor, Chapple & Stokes (1968) have pointed out that a cellular solution may exist. A cell is defined as a region between two neighbouring zero points of the function $H(\xi)$ that represents the axial component of the flow velocity. If $H(\xi) < 0$ then the fluid flows towards the lower disk, for $H(\xi) > 0$ the fluid flows to the upper disk. As a result the fluid cannot flow between cells. Each solution is characterized by the number of cells. Table 2 shows that the number of cells can change on a particular branch.

The function $F(\xi)$ represents a radial component of the velocity. For $F(\xi) < 0$ the

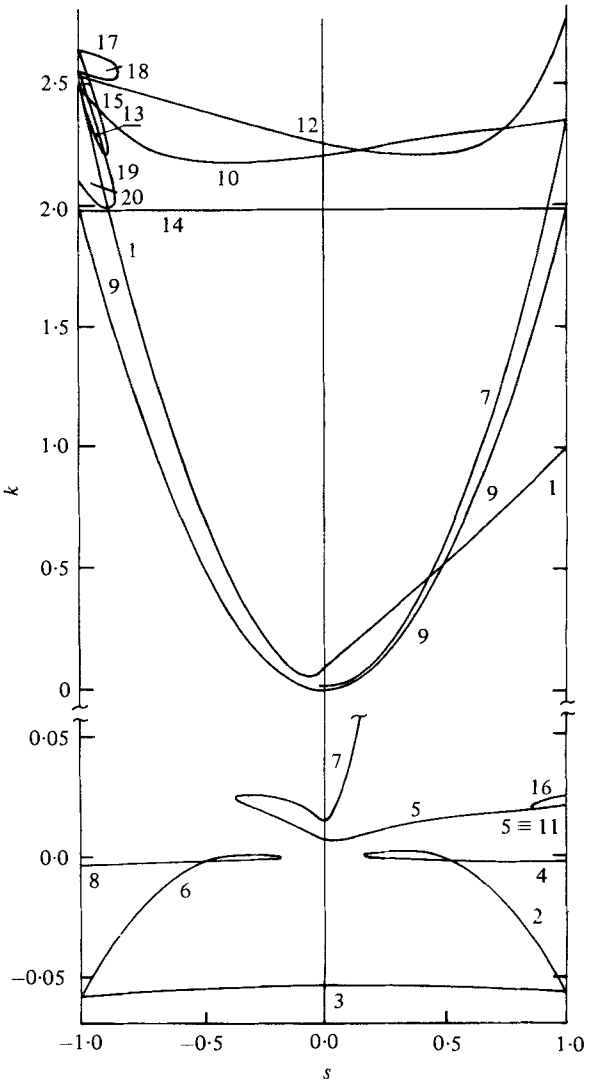

FIGURE 3. Dependence of k on the parameter s, $R = 625$.

fluid flows to the axis of the system (suction at the axis), for $F(\xi) > 0$ an outflow from the axis occurs. The angular component of the velocity is characterized by $G(\xi)$. For $G(\xi) > 0$ the fluid rotates in the same direction as the lower disk, for $G(\xi) < 0$ an opposite rotation results. Below we show the profiles $H(\xi)$, $F(\xi)$ and $G(\xi)$ on individual branches in figure 3 for three values of s. The following selected values of s represent the most interesting situation from the physical point of view:

(*a*) $s = 1$, both disks rotate with the same angular velocity (cf. figures 4*a–g*). The trivial solution (3) (branch 1) is not presented;

(*b*) $s = 0$, one disk does not rotate (cf. figures 5*a–h*);

(*c*) $s = -1$, both disks rotate with the same angular velocity but in opposite directions (cf. figures 6*a–h*).

Double-precision arithmetic ($\sim$ 15 decimal digits) has been used for all computations.

Branch (cf. figure 3)	Region s	Number of cells
1	1·0 to −0·4	1
	−0·45 to −0·6	3
	−0·65 to −1·0	2
2	1·0 to 0·2	2
3	1·0 to −1·0	2
4	1·0 to 0·165	2
5	1·0 to 0·15	2
	0·1 to −0·1	3
	−0·15 to −0·36	2
6	−0·17 to −1·0	2
7	1·0 to 0·7	2
	0·65	4
	0·6 to 0·2	3
	0·15 to −0·1	1
	−0·15	3
	−0·2 to −0·36	2
8	−0·2 to −1·0	2
9	1·0 to −1·0	1
10	1·0 to −0·85	2
	−0·9 to −1·0	4
11	1·0 to 0·851	2
12	1·0	6
	0·95	4
	0·9 to −1·0	2
13	−0·89665 to −0·9	2
	−0·95 to −1·0	4
14	1·0 to −1·0	1
15	−0·89665 to −1·0	2
16	1·0	4
	0·95 to 0·851	2
17	−0·858 to −1·0	2
18	−0·858 to −1·0	2
19	−0·859 to −1·0	2
20	−0·9 to −1·0	4
	−0·859 to −0·9	2

TABLE 2. Numbers of cells on different branches for certain regions of s; $R = 625$.

The grid number $n = 400$ has been adapted and all profiles are correct in the scale of the figures. Comments of the behaviour of the system are presented in the legends to the figures. Let us note that, for $s = 1$ and $s = -1$ and asymmetrical solutions, there exist also solutions constructed by using relations (4) and (5). The construction of streamlines is described in the paper by Batchelor (1951) and it is not difficult to draw the streamlines for individual cases.

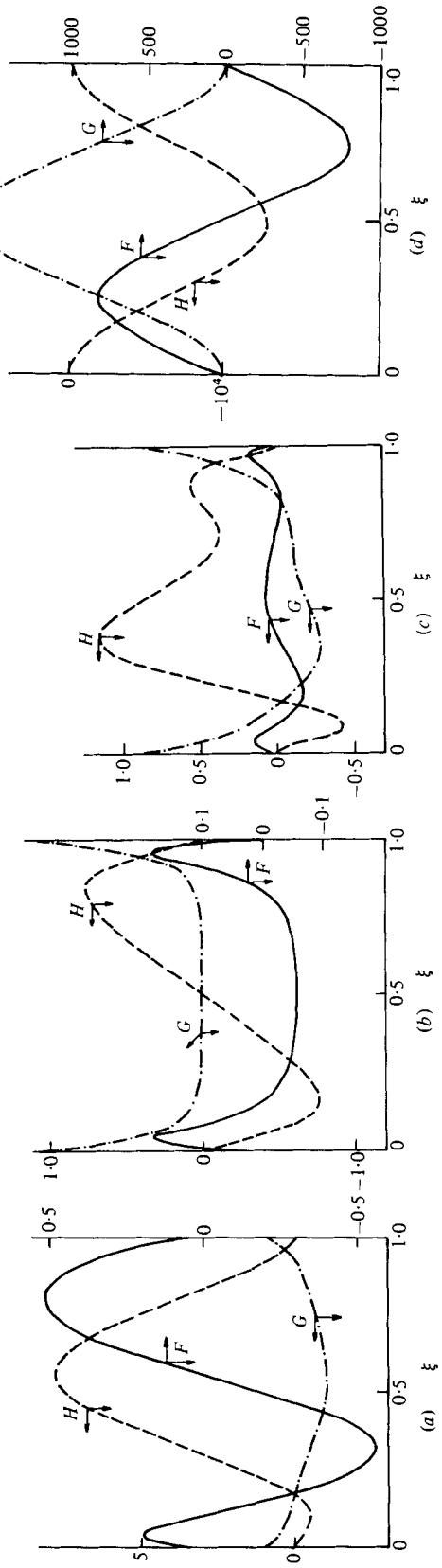

FIGURE 4. For legend see p. 237.

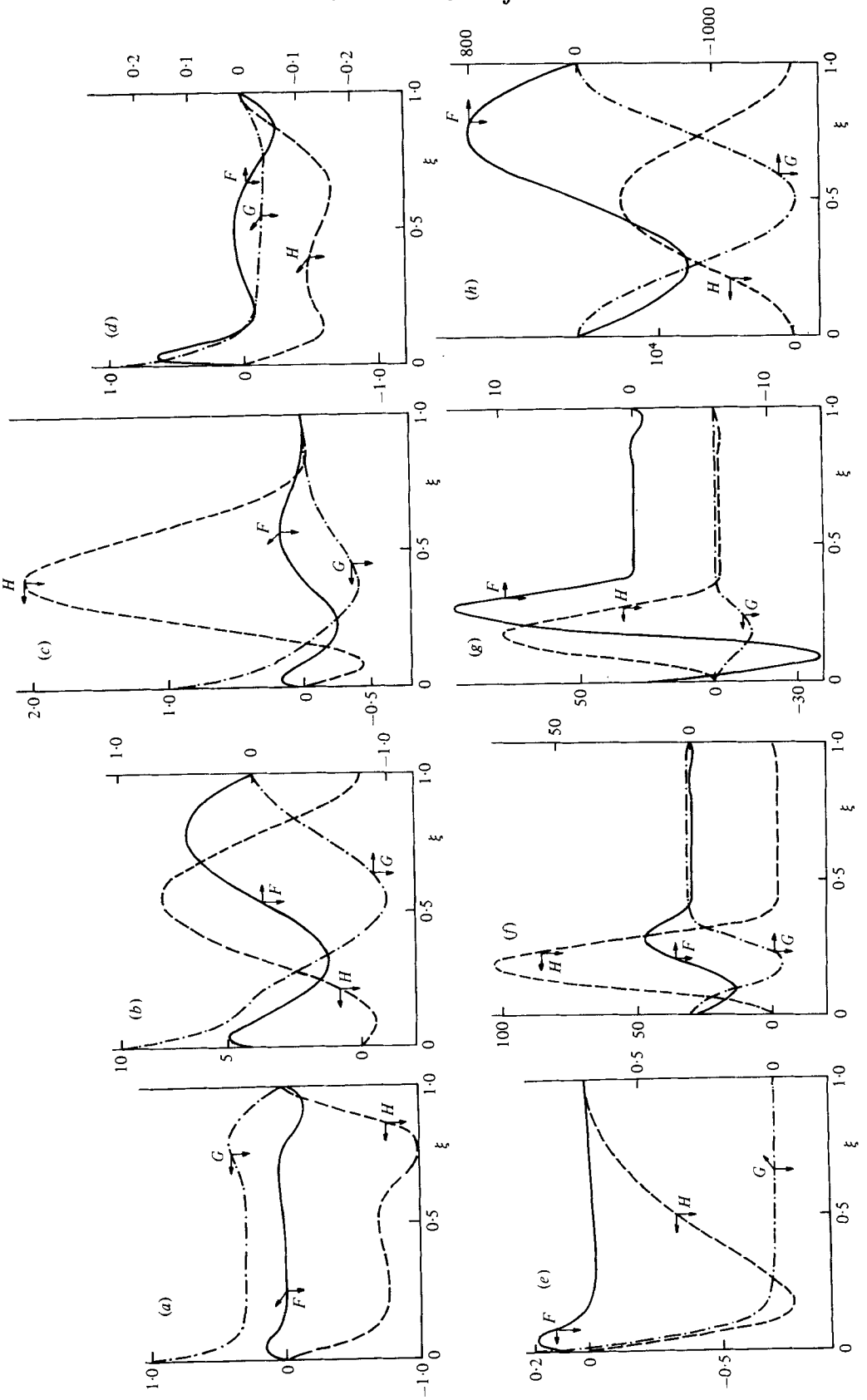

FIGURE 5. For legend see p. 237.

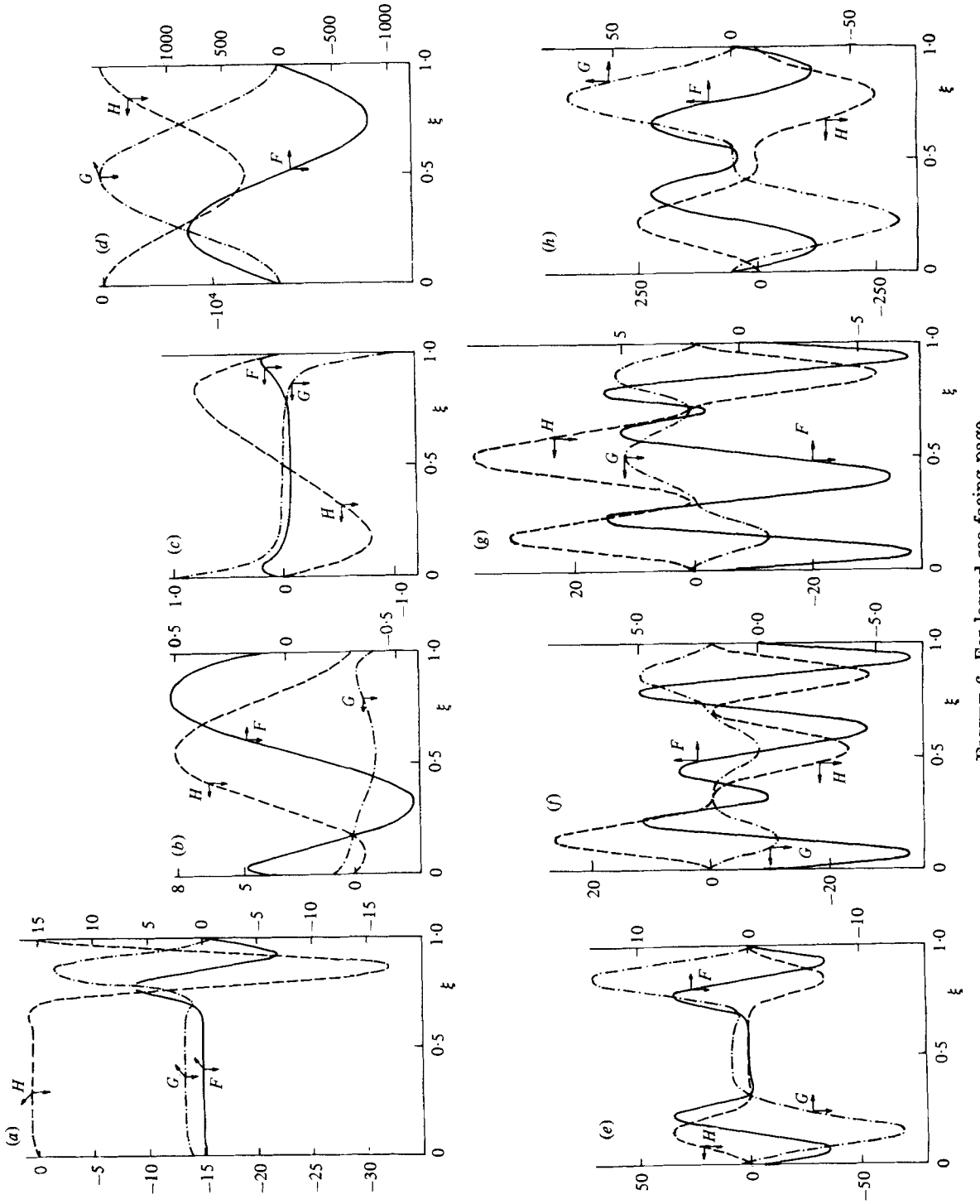

FIGURE 6. For legend see facing page.

LEGENDS TO FIGURES 4, 5 AND 6

FIGURE 4. Resulting profiles for $s = 1$. (*a*) Branch 3, $k = -0{\cdot}056366$, two cells. By using (4) we can obtain the solution for branch 2. A part of the fluid rotates with an opposite angular velocity; both disks behave as centrifuges; the outflow is not uniform; the flow is higher at one disk. (*b*) Branch 4, $k = -0{\cdot}002663$, two cells. Both disks behave as centrifuges; the fluid rotates only in a boundary layer; outside the boundary layer only a radial and axial flow results. (*c*) Branch 5, $k = 0{\cdot}020168$, two cells. By using (4) we can obtain the solution for branch 11. A part of the fluid rotates with an opposite angular velocity. A boundary layer appears at both disks with an outflow in radial direction. (*d*) Branch 9, $k = 1{\cdot}983135$, one cell. By using (4) we can obtain a solution for branch 14. The fluid rotates between very narrow boundary layers with high velocity. Rotation of the disks exerts only a weak effect on the behaviour of the fluid. One disk behaves as a centrifuge with an inflow in the axial direction; at the second disk the fluid is sucked. (*e*) Branch 10, $k = 2{\cdot}346506$, two cells. By using (4) we can obtain a solution for branch 7. Near one disk a layer of fluid exists which rotates with higher opposite velocity than both disks. The fluid is sucked in the radial direction and then flows out. (*f*) Branch 12, $k = 2{\cdot}738047$, six cells. There are layers rotating rapidly and in opposite directions at both disks. Between these layers the fluid rotates like a rigid body. (*g*) Branch 16, $k = 0{\cdot}023509$, four cells. Both disks behave as centrifuges; in the middle layer the fluid rotates with an opposite angular velocity and an outflow in the radial direction results.

FIGURE 5. Resulting profiles for $s = 0$. (*a*) Branch 1, $k = 0{\cdot}098264$, one cell. The fluid is sucked near the standing disk and flows in the radial direction. The rotating disk behaves as a centrifuge. (*b*) Branch 3, $k = -0{\cdot}053848$, two cells. The fluid rotates in the opposite direction near the standing disk and in the middle layer. A narrow boundary layer arises at the rotating disk where the disk behaves as a centrifuge. A radial inflow occurs in the middle layer and there is a radial outflow near the standing disk. (*c*) Branch 5, $k = 0{\cdot}006760$, three cells: a similar situation to that in (*b*). (*d*) Branch 7, $k = 0{\cdot}015180$, one cell. The fluid rotates in the opposite direction near the standing disk; nevertheless, the situation is similar to that in (*a*). There is a different behaviour in the middle layer where radial outflow and inflow take place. (*e*) Branch 9, $k = 0{\cdot}000040$, one cell. The rotating disk behaves as a centrifuge in a narrow boundary layer. The rest of the fluid does not rotate, only radial flow results. (*f*) Branch 10, $k = 2{\cdot}205886$, two cells. The fluid rotates in the opposite direction near the rotating disk. This effect causes a boundary layer analogously to figure 4(*e*). (*g*) Branch 12, $k = 2{\cdot}251744$, two cells. A layer rotating rapidly and in the opposite direction is constituted near the rotating disk. The rest of the fluid rotates as a rigid body. (*h*) Branch 14, $k = 1{\cdot}983135$, one cell. The velocities are so high that the situation is very similar to that in figure 4(*d*). The influence of the upper disk can be neglected.

FIGURE 6. Resulting profiles for $s = -1$. (*a*) Branch 1, $k = 2{\cdot}530180$, two cells. By using (5) we can obtain the solution on branch 12. The fluid rotates in the opposite direction near one disk (cf. figure 5*g*). Near the second disk the fluid is almost standing. (*b*) Branch 3, $k = -0{\cdot}057678$, two cells. By using (5) we can obtain a solution on branch 6. The situation is similar to figure 4(*a*), only the angular velocity is different. (*c*) Branch 8, $k = -0{\cdot}002956$, two cells. Both disks behave as a centrifuge with an inflow in the radial direction. (*d*) Branch 9, $k = 1{\cdot}983135$, one cell. By using (5) we can obtain the solution on branch 14. This situation is analogous to figure 4(*d*). (*e*) Branch 10, $k = 2{\cdot}494857$, four cells. By using (5) we can obtain a solution on branch 13. A layer of fluid rotating in the opposite direction is constituted near both disks. Solutions on branches 10 and 13 are for $s = -1$ very similar. (*f*) Branch 15, $k = 2{\cdot}646086$, two cells. By using (5) we can obtain a solution on branch 17. The fluid rotates in three layers with inflow and outflow in each of them. Near both disks a flow with an opposite angular velocity exists and an inflow near the disks occurs. (*g*) Branch 18, $k = 2{\cdot}548247$, two cells. By using (5) we can obtain a solution on branch 19. The flow is analogous to that in (*f*). (*h*) Branch 20, $k = 2{\cdot}063128$, four cells. Near both disks the fluid rotates with an opposite angular velocity. The radial inflow occurs near both disks and an outflow in the middle layer results.

4. Discussion

Batchelor (1951) constructed for $s = -1$ a solution which is composed of a boundary layer, a layer with constant angular velocity, an intermediate layer, a layer with constant angular velocity and a boundary layer. So far we have not observed this situation. In the case $s \geqslant 0$ Batchelor supposed that the disk with higher angular velocity behaves as a centrifuge while at the slower disk a suction effect occurs; this prediction is in agreement with our results (see figure 5*a*). He assumed that for higher values of the Reynolds number the fluid between boundary layers will rotate with a constant angular velocity (cf. figure 5*a*).

Stewartson (1953) compared Batchelor's conclusions with experiments. He used a power-series expansion (in R) to solve the boundary-value problem in question. Our results, presented in figures 6(*c*) and 5(*e*), are analogous to the results obtained by Stewartson.

Lance & Rogers (1962) described for $s = 0{\cdot}5$ and $R \in [1, 169]$ a situation when a layer of an almost stagnant fluid is surrounded by two boundary layers. Their calculations are related to our results in figures 5(*a*) and 6(*c*) for $s = 0$ and $s = -1$, respectively.

Pearson (1965) obtained for $s = 0$, $R = 100$ and 1000 solutions which are analogous to our figure 5(*a*). For $s = -1$ and $R = 100$ he obtained a symmetrical solution (cf. figure 6*c*); for $R = 1000$ he found a solution where the main part of the fluid rotates with a higher angular velocity than that of the particular disks (cf. figure 6*b*), branch 6). Mellor *et al.* (1968) solved the problem for $s = 0$ and calculated the dependence of the solution on the Reynolds number R. They found branches of the solution where two one-cell (cf. figure 5*a*), one two-cell and one three-cell (cf. figure 5*c*) configurations occur. Rasmussen (1971) and Tam (1969) solved the problem analytically, their results can be compared with our calculations only in a qualitative way. Greenspan (1971) analysed the problem for different values of parameters; for $s = -1$ and $R = 1000$ and 2000 there is a discrepancy between his results and the calculations of McLeod & Parter (1974). The corrected results which correspond to our figure 6(*c*) are presented in a later work (Schultz & Greenspan 1974). McLeod & Parter analysed the problem for $s = -1$ theoretically. They supposed *a priori* the symmetry of the solution. Their conclusions are in agreement with our results when the profiles are symmetrical. Unfortunately, the solutions can also be non-symmetrical and thus their theory cannot be used in these cases. The profiles presented for lower values of R ($R = 100$) by Barrett (1975) are identical with our results. The solution obtained by Nguyen, Ribault & Florent (1975) can be compared for the case of $s = 0$; they obtained for $R = 500$ and $R = 1000$ a solution of Batchelor (cf. figure 5*a*) and Stewartson (cf. figure 5*e*) type. The conclusion of Nguyen *et al.* was that the solution of Batchelor type is dynamically stable.

For $s = -1$, Pesch & Rentrop (1978) assumed symmetry of the profiles and calculated the solution within the halved interval. Their results agree with figure 6(*c*). For $s = 0$ Roberts & Shipman (1976) calculated a dependence of the solution on R. They obtained the branches calculated by Mellor *et al.* (1968) and found that the number of cells was constant on one particular branch.

There is a related problem which has been studied in the literature, namely the problem of only one rotating disk. Let us mention at least the papers by Dijkstra & Zandbergen (1976) and Zandbergen (1980), where two and infinitely many solutions of

the problem have been obtained, respectively. It would also be interesting to answer the question on the relation between the solutions for the one-disk and two-disk problems.

All solutions we have found are drawn in the figures. A description of each individual situation is presented in the legends to figures 4, 5 and 6. We have obtained a number of qualitatively different steady-state solutions of the problem. The stability of these solutions has not been tested; it will be the subject of our next paper. We have shown that a majority of the results published in the literature are consistent with our calculations. The results of the calculations indicate that for higher values of the Reynolds number the situation is quite complicated and that a great number of different branches exist. It is an open question whether or not we have evaluated all the possible branches for $R = 625$. We feel that there is a possibility that certain solutions have not yet been discovered. The results of our calculations revealed that with higher values of R the number of solutions increases.

A detailed analysis of the problem of finite disks with respect to the existence of multiple steady states has not yet been presented. Recently a preliminary analysis of finite disks has been published (Bodonyi & Stewartson 1977; Szeri & Adams 1978). In future work we should like to show the effect of finite dimensions of rotating disks on the qualitative behaviour of the problem considered. With respect to experimental evidence of complex hysteresis behaviour of two rotating cylinders (Coles 1965) it can be expected that, for rotating fluids, multiple steady states may occur.

The authors express their thanks to Dr Miroslava Schlehöferová for her assistance in computations.

REFERENCES

Barrett, K. E. 1975 Numerical study of the flow between rotating coaxial disks. *J. Appl. Math. Phys.* **26**, 807.

Batchelor, G. K. 1951 Note on a class of solutions of the Navier–Stokes equations representing steady rotationally symmetric flow. *Quart. Mech. Appl. Math.* **4**, 29.

Bodonyi, R. J. & Stewartson, K. 1977 The unsteady laminar boundary layer on a rotating disk in a counter-rotating fluid. *J. Fluid Mech.* **79**, 669.

Coles, D. 1965 Transition in circular Couette flow. *J. Fluid Mech.* **21**, 385.

Dijkstra, D. & Zandbergen, P. J. 1976 Non-unique solutions of the Navier–Stokes equations for the Kármán swirling flow. *Technische Hogeschool Twente, Memo.* Nr. 155.

Greenspan, D. 1971 Numerical studies of flow between rotating coaxial disks. *Univ. Wisconsin-Madison, Tech. Rep.* 110.

Holodniok, M., Kubíček, M. & Hlaváček, V. 1977 Computation of the flow between two rotating coaxial disks. *J. Fluid Mech.* **81**, 689.

Lance, G. N. & Rogers, M. H. 1962 The axially symmetric flow of a viscous fluid between two infinite rotating disks. *Proc. Roy. Soc.* A **266**, 109.

McLeod, J. B. & Parter, S. V. 1974 On the flow between two counter-rotating infinite plane disks. *Arch. Rat. Mech. Anal.* **54**, 301.

Mellor, G. L., Chapple, P. J. & Stokes, V. K. 1968 On the flow between a rotating and a stationary disk. *J. Fluid Mech.* **31**, 95.

Nguyen, N. D., Ribault, J. P. & Florent, P. 1975 Multiple solutions for flow between coaxial disks. *J. Fluid Mech.* **68**, 369.

Pearson, C. E. 1965 Numerical solutions for the time-dependent viscous flow between two rotating coaxial disks. *J. Fluid Mech.* **21**, 623.

Pesch, H. J. & Rentrop, P. 1978 Numerical solution of the flow between two-counter-rotating infinite plane disks by multiple shooting. *Z. angew. Math. Mech.* **58**, 23.

RASMUSSEN, H. 1971 High Reynolds number flow between two infinite rotating disks. *J. Australian Math. Soc.* **12**, 483.

ROBERTS, S. M. & SHIPMAN, J. S. 1976 Computation of the flow between a rotating and a stationary disk. *J. Fluid Mech.* **73**, 53.

SCHLEHÖFEROVÁ, M., HOLODNIOK, M. & KUBÍČEK, M. 1981 Dependence of the solution of nonlinear boundary value problems on a parameter by multiple shooting. *Num. Math.* (to be published).

SCHULTZ, D. & GREENSPAN, D. 1974 Simplification and improvement of a numerical method for Navier–Stokes problems. *Univ. Wisconsin-Madison, Tech. Rep.* 211.

STEWARTSON, K. 1953 On the flow between two rotating coaxial disks. *Proc. Camb. Phil. Soc.* **49**, 333.

SZERI, A. Z. & ADAMS, M. L. 1978 Laminar throughflow between closely spaced rotating disks. *J. Fluid Mech.* **86**, 1.

TAM, K. K. 1969 A note on the asymptotic solution of the flow between two oppositely rotating infinite plane disks. *SIAM J. Appl. Math.* **17**, 1305.

ZANDBERGEN, P. J. 1980 *New Solutions of the Kármán Problem for Rotating Flows*, Lecture Notes in Mathematics, vol. 771. Springer.